Stem Cell Research (2014) 12, 730–741

Available online at www.sciencedirect.com

ScienceDirect

www.elsevier.com/locate/scr

Mechanistic elements and critical factors of cellular reprogramming revealed by stepwise global gene expression analyses

Sung-Jin Park[a,1], Hock Chuan Yeo[b,1], Nam-Young Kang[a,1], Hanjo Kim[c,2], Joyce Lin[b], Hyung-Ho Ha[c,3], Marc Vendrell[a,4], Jun-Seok Lee[c,5], Yogeswari Chandran[a], Dong-Yup Lee[b,d,*], Seong-Wook Yun[a,**], Young-Tae Chang[a,c,***]

[a] *Laboratory of Bioimaging Probe Development, Singapore Bioimaging Consortium, Agency for Science, Technology and Research, Singapore 138667, Republic of Singapore*
[b] *Bioinformatics Group, Bioprocessing Technology Institute, Agency for Science, Technology and Research, Singapore 138668, Republic of Singapore*
[c] *Department of Chemistry & NUS MedChem Program of Life Sciences Institute, National University of Singapore, Singapore 117543, Republic of Singapore*
[d] *Department of Chemical and Biomolecular Engineering, National University of Singapore, Singapore 117576, Republic of Singapore*

Received 31 May 2013; received in revised form 21 February 2014; accepted 17 March 2014
Available online 25 March 2014

Abstract A better understanding of the cellular and molecular mechanisms involved in the reprogramming of somatic cells is essential for further improvement of induced pluripotent stem (iPS) cell technology. In this study, we enriched for cells actively undergoing reprogramming at different time points by sorting the cells stained with a stem cell-selective fluorescent chemical

Abbreviations: CDy1, compound of designation yellow 1; DEG, differentially expressed gene; FDR, false discovery rate; OSKM, Oct4, Sox2, Klf4, c-Myc; PDGF, platelet derived growth factor.

* Correspondence to: D.-Y. Lee, Department of Chemical and Biomolecular Engineering, National University of Singapore, Singapore 117576, Republic of Singapore. Fax: +65 6779 1936.
** Correspondence to: S.-W. Yun, Laboratory of Bioimaging Probe Development, Singapore Bioimaging Consortium, Agency for Science, Technology and Research, Singapore 138667, Republic of Singapore. Fax: +65 6478 9957.
*** Correspondence to: Y.-T. Chang, Department of Chemistry & NUS MedChem Program of Life Sciences Institute, National University of Singapore, Singapore 117543, Republic of Singapore. Fax: +65 6516 1691.
E-mail addresses: cheld@nus.edu.sg (D.-Y. Lee), yun_seong_wook@sbic.a-star.edu.sg (S.-W. Yun), chmcyt@nus.edu.sg (Y.-T. Chang).
URL: http://ytchang.science.nus.edu.sg (Y.-T. Chang).
[1] These authors contributed equally to this work.
[2] Present address: R&D Centre, EQUISnZAROO Co., Ltd., Seongnam 463-400, Republic of Korea.
[3] Present address: College of Pharmacy, Sunchon National University, Sunchon 540-742, Republic of Korea.
[4] Present address: MRC Centre for Inflammation Research, Queen's Medical Research Institute, University of Edinburgh, EH16 4TJ, UK.
[5] Present address: Future Convergence Research Division, Biomolecules Function Research Centre, Korea Institute of Science and Technology, Seoul 136-791, Republic of Korea.

http://dx.doi.org/10.1016/j.scr.2014.03.002

probe CDy1 for their global gene expression analysis. Day-to-day comparison of differentially expressed genes showed highly dynamic and transient gene expressions during reprogramming, which were largely distinct from those of fully-reprogrammed cells. An unbiased analysis of functional regulation indicated robust modulation of concurrent programs at critical junctures. Globally, transcriptional programs involved in cell proliferation, morphology and signal transduction were instantly triggered as early as 3 days-post-infection to prepare the cell for reprogramming but became somewhat muted in the final iPS cells. On the other hand, the highly coordinated metabolic reprogramming process was more gradually activated. Subsequent network analysis of differentially expressed genes indicated PDGF-BB as a core player in reprogramming which was verified by our gain- and loss-of-function experiments. As such, our study has revealed previously-unknown insights into the mechanisms of cellular reprogramming.

Introduction

Since the first report of induced pluripotent stem (iPS) cells generated by the expression of four transcription factors Oct4, Sox2, Klf4 and c-Myc (OSKM) in fibroblasts (Takahashi and Yamanaka, 2006), there has been a variety of technical improvements to generate iPS cells more efficiently. Different combinations of reprogramming transcription factors or addition of synthetic chemicals that influence epigenetic regulation and signaling pathways have been discovered to enhance the reprogramming efficiency and quality of stem cells (Feng et al., 2009b; Han et al., 2010; Lin et al., 2009). However, the mechanism of reprogramming, especially at the early phases, remains elusive. One of the reasons for the scant knowledge about reprogramming mechanisms is the very low efficiency of reprogramming. Only a small number of cells, which is undergoing reprogramming, need to be isolated out of heterogeneous cell populations for the analysis. Although the expression of fluorescent proteins using Oct4 or Nanog promoters has been used to detect and isolate mature iPS cells in 2–4 weeks of time, there has been no efficient way to probe the cells undergoing reprogramming at early phases. Profiling gene expression patterns during reprogramming has previously been attempted using unsorted mixed populations of secondary mouse embryonic fibroblasts (MEFs) harboring doxycycline-inducible OSKM genes (Samavarchi-Tehrani et al., 2010) or partially reprogrammed cell lines which were not actively undergoing reprogramming (Mikkelsen et al., 2008). Recently, Buganim et al. identified single cells which turn into iPS cells and analyze expression profiles of 48 genes in those cells (Buganim et al., 2012), while Polo et al. analyzed global gene expression profiles of the cells enriched based on SSEA-1 and Thy1 expressions (Polo et al., 2012) and Hansson et al. analyzed proteome changes during reprogramming under dox-inducible transgenic system (Hansson et al., 2012). The reprogramming mechanisms newly revealed by these studies demonstrate the necessity of more tools with which the rare cells undergoing reprogramming can be isolated.

We previously reported a fluorescent chemical probe CDy1, which selectively stains living embryonic stem (ES) cells of both human and mouse origin and enables the isolation of ES cells from a mixture with fibroblasts by fluorescence-activated cell sorting (FACS) (Im et al., 2010; Kang et al., 2011). CDy1 detects iPS cells as well, at both early and late phases of reprogramming as demonstrated using the cells of a transgenic mouse that express GFP under the control of Oct4 promoter. When the mouse fibroblasts were transfected with retroviral vectors encoding OSKM and then incubated with CDy1, some colonies were brightly stained at 10 days post infection (dpi) before GFP expression, which eventually turned into GFP-expressing colonies at a later time. In another study, we demonstrated that CDy1 can be used as an iPS cell reporter even at 7 dpi in a high throughput screening of chemicals designed for the development of reprogramming enhancer (Vendrell et al., 2012). These findings led us to hypothesize that cells undergoing reprogramming could be isolated at different time points during reprogramming using CDy1 and their stepwise global gene expression analysis would enable the identification of key mechanisms, pathways or molecules that play important roles in cellular reprogramming. Based on this hypothesis, we identified differentially expressed genes (DEGs) in the CDy1-positive cells harvested at several early time points of reprogramming starting from as early as 3 dpi and analyzed the data using various bioinformatics tools. A functional transcriptomic analysis of the data revealed an unprecedented sequence of cellular mechanisms of reprogramming and a DEG network analysis identified PDGF-BB as a critical factor for the process.

Materials and methods

Cell culture

MEFs were cultured on gelatin-coated dish in high-glucose Dulbecco's Modified Eagle's medium (DMEM) supplemented with 10% fetal calf serum, 2 mM L-glutamine, 100 U/ml penicillin, 100 μg/ml streptomycin, 0.1 mM non-essential amino acids and 0.1% β-mercaptoethanol. To be used as feeder, the cells were treated with mitomycin C (10 μg/ml) for 2 h and washed with PBS. iPS cells were cultured on these feeder cells in DMEM containing 20% knock-out serum replacement (KOSR, Invitrogen), 1 mM L-glutamine, 0.1 mM β-mercaptoethanol, 1% non-essential amino acids and 100 U/ml leukemia inhibitory factor (LIF, Chemicon).

iPS cell generation

MEFs prepared from B6;CBATg(Pou5f1-EGFP)2Mnn/J mouse (Jackson Laboratory) were infected by pMX-Oct4, Sox2, Klf4 and c-Myc expressing retrovirus with 10 μg/ml polybrene (Sigma) in normal MEF culture medium for 1 day and the medium was replaced with iPS cell culture medium the next day (1 dpi). At 2 dpi, the infected cells were seeded on

30,000 cells/well feeder cells at a density of 10,000 cells/well in 12-well plates. The medium was replaced daily and Oct4-GFP positive colonies were counted from the fluorescence images taken at 24 dpi using an ImageXpress^{MICRO} system.

Fluorescence-activated cell sorting

Cells incubated with 100 nM of CDy1 for 1 h were washed with PBS and harvested using trypsin-EDTA. Since unhealthy and dead cells are non-selectively stained by CDy1, living cells were gated based on side and forward scatter profiles before collecting cells. At least 8×10^5 cells from the 7% of living cells at the bright side of PE-Texas Red fluorescence histogram were collected using FACS Aria™ (BD Biosciences). For each reprogramming time point analyzed, 2 sets of cell samples were collected from independent experiments.

DNA microarray profiling, pre-processing and differential expression analysis

The total RNA was extracted from 8×10^5 cells/sample to synthesize cRNA using an Illumina TotalPrep RNA amplification kit. Purified and labeled cRNA was hybridized onto MouseRef-8 v2 Expression BeadChips (Illumina) in duplicate according to the manufacturer's instructions. The bead intensities were mapped to gene information using BeadStudio 3.2 (Illumina), and underwent variance stabilizing transformation and robust spline normalization in the R's Lumi package. Correlation scatter plots and hierarchical clustering were done using GenPlex software package (Istech).

We used an online tool (Laing and Smith, 2010) based on the rank product algorithm (Breitling et al., 2004) for differential expression analysis of the microarray data. A major strength of this approach is the lower number of replicates required for similar false discovery rates, compared to analyses requiring some variation of standard deviation computation. Importantly, the algorithm requires a minimum of two replicates for the q-value (corrected p-value) evaluation of transcript probe compared to three replicates for approaches based on statistical deviation computation. As such, we were able to use q-value which is an objective and more reliable criterion in short-listing genes for further analysis compared to the commonly-used simple fold-change. Venn diagram analyses of DEGs were done online (VENNY: http://bioinfogp.cnb.csic.es/tools/venny/index.html).

Functional regulation based on enrichment analysis

Gene enrichment analysis based on the tool in the DAVID database (Huang da et al., 2009) was conducted on DEGs to shortlist interesting molecular and functional events from both parental-MEF comparisons and sequential comparisons. A modified Fisher's exact p-value (EASE score) of 1.0 is assigned for under-representation of differentially-expressed genes in gene groups. All gene groups with $-\log10$ (modified p-value) >2.0 for any early reprogramming days were preliminarily shortlisted from KEGG's pathway, PANTHER's pathway and GO's biological process (FAT) databases and then assigned to major functional categories. Interesting functional phenomena that were further studied typically had $-\log10$ (modified p-value) much greater than 2.0 for involved gene groups and their analyses were exhaustively augmented with knowledge on reprogramming biology. In the process, complementary, synergistic and antagonistic gene groups are also used to help understand the detailed mechanisms of the broader function. In doing so, we used the enrichment significance of a gene group as a numerical proxy for measuring the corresponding functional regulation over time, providing information on regulation onsets, time spans and maxima. By combining usage of both parental-MEF and sequential comparisons in regulation study, we tracked changes from different angles, both of which contributed understanding to the physiological process of interest.

Functional regulation of major categories

To assess functional regulation of major functional categories, memberships of participating gene groups were consolidated and its enrichment of differentially-expressed genes was recomputed using Fisher's exact test (http://www.langsrud.com/fisher.htm) in a collated fashion.

Network analysis

The gene lists were uploaded to IPA database to overlay eligible molecules onto a global molecular network developed from information contained in the Ingenuity Knowledge Base. Networks of network eligible molecules were then algorithmically generated based on their connectivity through the use of IPA (Ingenuity® Systems, www.ingenuity.com).

Real time RT-PCR

The total RNA was extracted from 1×10^6 cells/sample using RNeasy Mini Kit (QIAGEN) according to the manufacturer's instruction. One-step quantitative RT-PCR was performed on a StepOne™ Real-Time PCR System using a Power SYBR® Green RNA-to-CT™ 1-Step Kit (Applied Biosystem). The relative mRNA levels of the genes of interest were normalized to that of GAPDH. The primer sequences used in this study are listed in Supplementary Table 1.

PDGFR inhibitor and PDGF-BB antibody treatment

Various concentrations of AG 17 (Merck), AG 1295 (Merck), AG 1296 (Merck) and Gleevec (Novartis) were added into the medium from 3 dpi to 24 dpi. For PDGF neutralization experiment, PDGF-BB antibody (Abcam) was added from 3 dpi to 24 dpi.

In vitro differentiation of iPS cell

Embryoid bodies were generated by culturing iPS cells for 3 days in low-adherent dishes using a high-glucose DMEM supplemented with 10% fetal calf serum, 2 mM L-glutamine, 100 U/ml penicillin, 100 μg/ml streptomycin, 0.1 mM non-essential amino acids and 0.1% β-mercaptoethanol. Embryoid bodies were seeded on gelatin coated plates and further cultured for 10 days for differentiation in the same media as used for embryoid body generation.

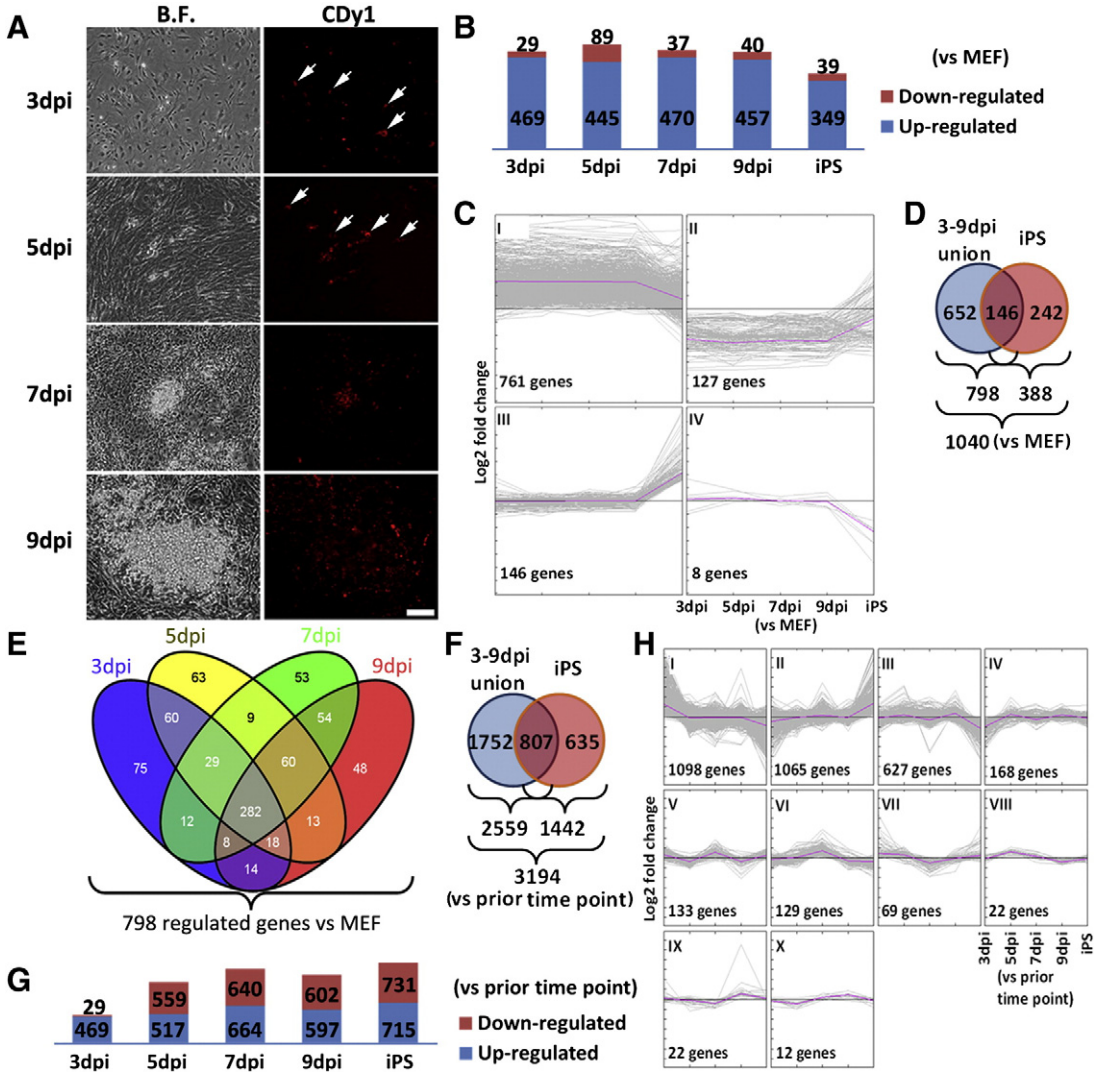

Figure 1 Global gene expression profiles during reprogramming. (A): CDy1-stained distinct cell populations in OSKM-factor transfected MEF were observed using fluorescence microscopy at 3, 5, 7 and 9 dpi of reprogramming. Left panels, bright field phase contrast images; right panels, fluorescence images. CDy1-stained cells at 3 and 5 dpi are marked with white arrows. Scale bar, 100 μm. (B): The numbers of up- or down-regulated genes at each sample day at FDR ≤ 0.25 compared to the levels in fibroblast. (C): Fold change profiles of 4 main gene clusters identified using K-median clustering with dot product metric. Total gene count is greater than 1040 as a small number of genes had both up- and down- regulated transcript probes. (D): The number of genes whose expression levels were regulated at FDR ≤ 0.25 compared to the levels in fibroblast during reprogramming and in final iPS cell. (E): The number of genes whose expression levels were regulated at FDR ≤ 0.25 compared to the levels in fibroblast at specific sampled days during reprogramming. (F): The number of genes whose expression levels were regulated at FDR ≤ 0.25 compared to the levels at a prior time point. (G): The number of up- or down-regulated genes at each sample day at FDR ≤ 0.25 obtained using prior time-point comparison. (H): Gene expression dynamics during reprogramming obtained by K-median clustering based on dot product metric using prior time-point comparison.

Teratoma assay

Cells prepared in PBS were injected subcutaneously into the lower flanks of 8 weeks old SCID mice (3×10^6 cells in 0.15 ml per site). Tumors grown under the skin were excised 6–8 weeks after injection and fixed in 4% PFA for paraffin embedding, sectioning and H&E staining. All animal experiment procedures were performed in accordance with a protocol approved by the Institutional Animal Care and Use Committee.

Results

Dynamic and transitional gene expression profile during reprogramming

When the transfected MEFs were incubated with CDy1, scattered single cells stained by CDy1 were observed as early as at 3 dpi and morphologically distinguishable CDy1-stained colonies appeared from 7 dpi (Fig. 1A), which started to express GFP from 11 to 14 dpi (Supplementary Fig. S1A). We

collected the CDy1-stained brightest 7% of the cells, which was the minimum amount for the global gene expression analysis by DNA microarray, at 3, 5, 7 and 9 dpi using FACS. The cells were further characterized by assessing the expression of a pluripotent stem cell marker SSEA-1 and the capability of iPS cell colony formation. The percentages of SSEA-1$^+$ cells determined by flow cytometry gradually increased from 0.5% at 3 dpi to 1.7% at 9 dpi, which corresponded to 7.1% and 24.3% of the collected CDy1^{bright} cells. Almost 100% of SSEA-1$^+$ cells were identified as CDy1^{bright} cells at all time points (Supplementary Fig. S1B). The numbers of iPS cell colonies generated from CDy1^{bright} cells were significantly larger (2.6–9.1 fold) than those from CDy1^{dim} cells at all time points (Supplementary Fig. S2). These results suggest that CDy1 stains cells by detecting an earlier event in reprogramming than SSEA-1 and Oct4 expressions.

Parental MEF, an established iPS cell line and a mouse ES cell line were included as references. The lists of DEGs during reprogramming were obtained by comparing the data with that of MEF or prior time point cells using the rank product algorithm. For further analyses, we identified top-ranking DEGs using a false discovery rate (FDR) ≤ 0.25. Although the FDR threshold seems low conventionally, we noted that, with duplicates, we have rigorously controlled false gene discoveries by judiciously applying the rank product algorithm. The genes identified by the comparison to the expression levels of MEF were found to be mainly up-regulated during reprogramming and in the fully reprogrammed iPS cells with up-regulated genes 5–16 times as many as down-regulated ones (Fig. 1B), while similar ratios between up- and down-regulated genes were shown when identified by simple 2-fold change criteria (Supplementary Fig. S3A). A K-median clustering with average dot-product as metric identified 4 major regulation profiles which were remarkably distinguishable by the intermediate and established phases of reprogramming. They are: I) up-regulation during reprogramming which then moderated in final iPS cell; II) down-regulation during reprogramming which then also moderated in final iPS cell; III) up-regulation in final iPS cell only and; IV) down-regulation in final iPS cell only (Fig. 1C). Most early responding genes as exemplified by clusters I and II became mitigated in their regulation in final iPS cell, while genes with more moderated differential expression during reprogramming (clusters III and IV) tended to show greater fold changes in final iPS cell. Remarkably, genes in clusters I and II have highly similar kinetic profiles to that of Oct4, Sox2 and Klf4 transcription factors (Hansson et al., 2012), indicating that a substantial proportion of these genes are immediate targets of the factors. Interestingly, there were twice as many DEGs during the reprogramming timeframe compared to the fully reprogrammed cell (Fig. 1D). Furthermore, the expression of regulated genes continuously evolved in a transient manner during reprogramming. Specifically, only 35% (282/798) of DEGs identified during reprogramming were common to all 4 sampled days while another 30% (239/798) were highly specific to each day (Fig. 1E), indicating a high turnover of sharply-regulated genes.

With an eye for further elucidation of reprogramming dynamics, we rationalized that comparison of expression profiles to a prior time point i.e., 3 dpi vs. MEF, 5 dpi vs. 3 dpi, 7 dpi vs. 5 dpi, 9 dpi vs. 7 dpi and iPS cell vs. 9 dpi should directly trace the evolution of expression changes during reprogramming. This comparison revealed three times as many DEGs as the comparisons to MEF (3194 vs. 1040) at the same FDR level of ≤ 0.25 (Fig. 1F). Interestingly, the numbers of DEGs at 5, 7 and 9 dpi were approximately 10 times larger than those identified by simple 2-fold change criteria (Supplementary Fig. S3B). Notably, down-regulated genes were comparable in numbers to up-regulated ones in contrast to their relatively much smaller numbers from the comparisons to MEF (Fig. 1G). We noted that the larger number of transiently-regulated genes derived from prior-time-point comparisons did not translate into similar number of cumulatively-regulated genes from MEF comparisons for two reasons. These transient genes were either (1) changing expression level incrementally with a smaller fold-change or (2) alternating between up and down-regulation day-to-day as seen from multiple profiles of the K-means clustering result (Fig. 1H). Importantly, the expression changes for these genes are as significant (same FDR) (Supplementary Data 1), albeit with a smaller fold-change. They could be thought of as mainly providing an exploratory trajectory, in contrast to that of the highly regulated genes determining transitory phenotypes from MEF-comparisons. Secondly, we observed visually an anti-correlation between early (3 dpi vs. MEF) and late expression changes (iPS vs. 9 dpi) for most genes, as depicted in clusters I and II of Fig. 1H. This temporal switch-like-response of the transcriptome (from negative to positive regulation and vice-versa) was similarly observed earlier as the 'drastic resetting of the proteome' (Hansson et al., 2012). Overall, both our DEG clustering results for MEF and prior-time-point comparisons also revealed that most regulatory changes occurred either immediately following OSKM transfection (≤ 3 dpi) or during late phase of reprogramming (after 9 dpi).

Global analysis of cellular and molecular event

Functional enrichment analysis of DEGs is highly useful revealing the repertoire of significant events spanning various facets of the cell. Previous works by the others have sought to describe the kinetic expression profiles of selected functional genes or proteins during reprogramming. Moving one step upstream, we adopted an unbiased approach in evaluating global functional regulation by consolidating the memberships of significant gene groups that are associated with DEGs (Supplementary Fig. S4). From our results, we highlighted 4 major functional categories (Fig. 2) which showed striking similarities to trends reported in earlier studies, thus supporting their results. For example, genes with functions related to proliferation (Mikkelsen et al., 2008), and proteins related to morphology (and motility) (Hansson et al., 2012) showed immediate and abrupt regulation at 3 dpi which became mitigated in the fully-reprogrammed cells compared to MEF. Interestingly, our analysis revealed a more moderated increase in global metabolic regulation peaking at 9 dpi, which is surprisingly consistent with the more gradual expression of metabolic proteome (Hansson et al., 2012). More subtly, we noticed a good degree of correlation between the global proliferation and metabolism regulation profiles in MEF-comparisons (Fig. 2), with 3 dpi as an exception where the spike in proliferation regulation can be attributed to the reactionary response of OSKM expression. Importantly, the global signaling pathways were revealed for the first time to

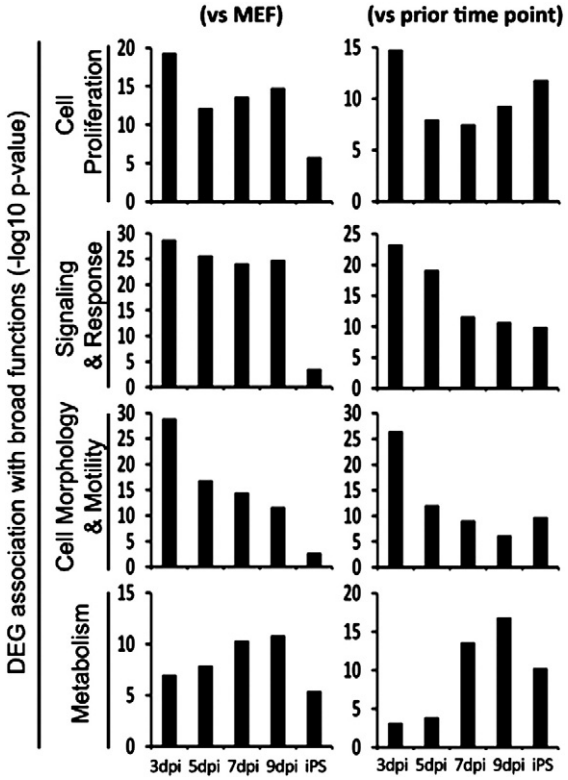

Figure 2 Relative associations of DEGs with major functions during reprogramming and in fully reprogrammed iPS cells. Left panels, comparison to the levels in MEF; right panels, comparison to the levels at the prior time point.

show a similarly abrupt and transient regulation profile which decreases significantly in the final iPS, underlying its importance as an early reprogramming mechanism.

Critical role of signaling in cell proliferation during the early phase of reprogramming

One canonical theme behind reprogramming efficiency is that rapid cell proliferation provides a key driving mechanism in reprogramming (Kawamura et al., 2009; Utikal et al., 2009). Due to the fundamental role of proliferation, we characterized the function globally and further investigated the molecular mechanisms for proliferation rate increase. Growth factor-mediated signal transduction has been demonstrated to be critical for cellular reprogramming as well as for pluripotent stem cell maintenance and differentiation (Miki et al., 2011; Silva et al., 2008; Wang et al., 2011). Our analysis which revealed early significant activation of signaling-related genes led us to hypothesize that signal transduction via membrane receptors may be employed as an active mechanism to initiate increased proliferation. We evaluated specific examples of DEGs involved in signal transduction and found the genes involved in various membrane receptor kinase signaling such as Bmp4, Fgf7, Fgf10, Fgf13, Tgfb3, Tgfbr2, Ltbp1, Ltbp3, and Pdgfra that are upstream of a similarly more active MAPK pathway modulating cell proliferation (Hoch and Soriano, 2003; Lanner and Rossant, 2010; Orford and Scadden, 2008) (Fig. 3A; Supplementary Fig. S4). As deduced from the combined effect of c-Myc trans-activation and increased signaling promoting mitogenesis, we found a resulting greater than 9-fold increase in cyclin D expression peaking at 7 dpi which drives resting fibroblasts through the restriction point (R) as well as G1/S transition. Consequently, these cells are likely to shorten their G1 gap phase as a first step towards reprogramming.

However, oxidative stresses generated during increased cell divisions can induce DNA damage and hence trigger the P53 pathway, potentially limiting the proliferation and reprogramming efficacy of aberrant cells. We found significant P53 pathway activity throughout early phases of reprogramming (Fig. 3A) with responding genes to support the notion of increased apoptotic sensitivity to DNA damage and also increased cell cycle arrest-induced repair. This include the activation of Cdkn1a, Cdkn2a, Trp53 identified in earlier studies (Kawamura et al., 2009; Marion et al., 2009; Mikkelsen et al., 2008; Utikal et al., 2009), and in addition, we found Scotin, Thbs1, Fas and Gadd45b/g to be similarly up-regulated. Accordingly, some cell cycle facilitators such as Cdc2a, Ccnb1 and Cdk2 were found to be down-regulated (Supplementary Fig. S4). It was unclear earlier as to the specific mechanisms of how proliferating cells are able to escape these anti-proliferation mechanisms during reprogramming. However, from our expression analysis of the control modules in the P53 pathway, the constitutive increase in cyclin D and Mdm2 levels appears to be cornerstones of increased proliferation, by bypassing cell cycle checkpoints in successfully reprogramming cells (Figs. 3B and C). For instance, due to the programs strongly driving cyclin D production, it is likely that the increase in P16 (Cdkn2a product) level could not effectively inhibit the mitogenic activities of cyclin D/Cdk complexes while P21 (Cdkn1a product) had a lesser propensity to induce cell cycle arrests being sequestered by higher levels of the same cyclin D/Cdk complexes. Similarly, high P53 and Arf (Cdkn2a product variant) expressions were also countered by a higher level of Mdm2 modulating P53 activation of cell cycle arrests, senescence or apoptosis. Upon full reprogramming, cells were released from stringent cell cycle checkpoints by the repression removal of Cdkn1a and Cdkn2a expression, while cell cycle facilitators such as Cdc2a and Ccnb1 were re-expressed (Figs. 3B and C). Our analysis also showed intense and rapid activation of hypoxia related genes at early reprogramming phase (Fig. 3A; Supplementary Fig. S4), which is in accordance with the finding that hypoxia improves reprogramming efficiency (Yoshida et al., 2009). Interestingly, most of these pathways became less significantly regulated in fully reprogrammed iPS cells. In all, these results suggested that genes for acceleration as well as inhibition of cell proliferation are both activated during the early phase of reprogramming due to increased signaling as well as proliferation-induced stresses. To this end, a switch-like rewiring of global signaling pathways in reprogramming cells compared to the final iPS cells was apparent from our analysis.

Ordered metabolic gene expressions at late phase of reprogramming

We reasoned that since a number of cell proliferation related gene groups showed consistent regulations that

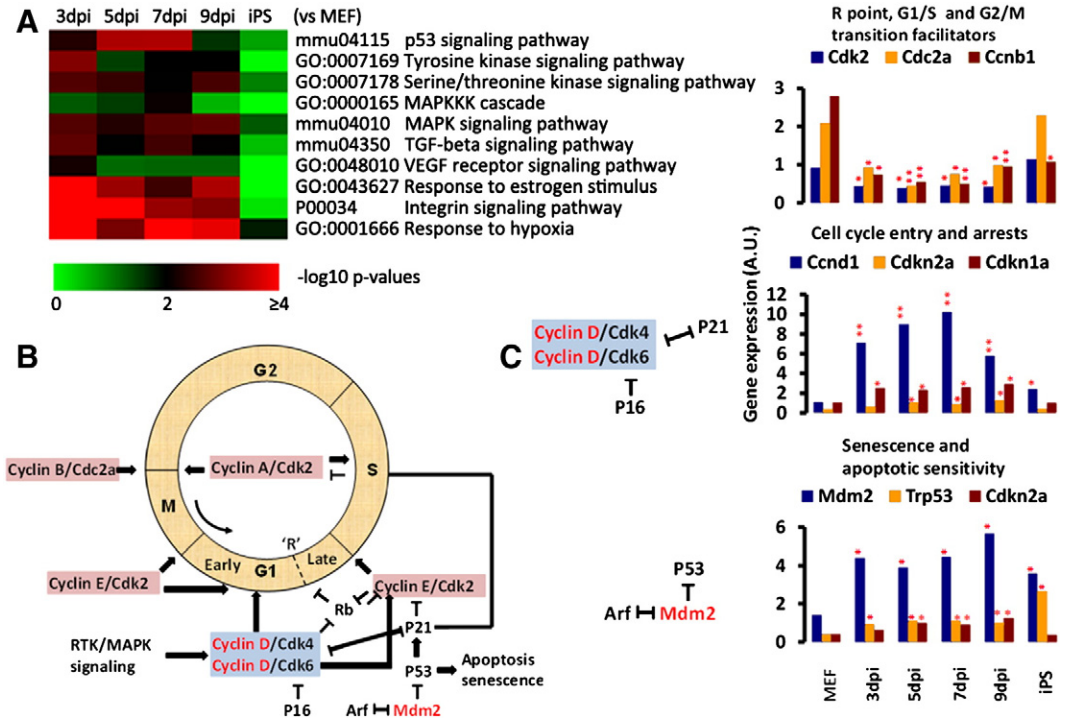

Figure 3 Transitional rewiring of global signaling network during early reprogramming. (A): Enrichment analysis reveals significant regulation of signaling pathways with switch-like regulation behavior between the cells undergoing reprogramming and the final iPS cell. (B): Diagram depicting molecular mechanisms involved in regulating proliferation by various pathways. It explains the effect of key genes in the P53 pathway on proliferation. Blue boxes indicate Cdk activities during reprogramming while red boxes indicate Cdk activities in both reprogramming and final iPS cells. (C): Key DEGs and control modules of the P53 pathway affect cell cycle facilitation, cell cycle arrests as well as senescence & apoptotic sensitivity during reprogramming. '*' and '**' represent a change in expression of at least two-folds and four-folds over MEF respectively. Although P53 pathway activators (Cdkn1a, Cdkn2a and Trp53) undergo significant increase and some cell cycle facilitators (Ccnb1, Cdc2a and Cdk2) are down-regulated, the constitutive increase in cyclin D and Mdm2 negates the effects of cell proliferation inhibitors in successfully reprogramming cells.

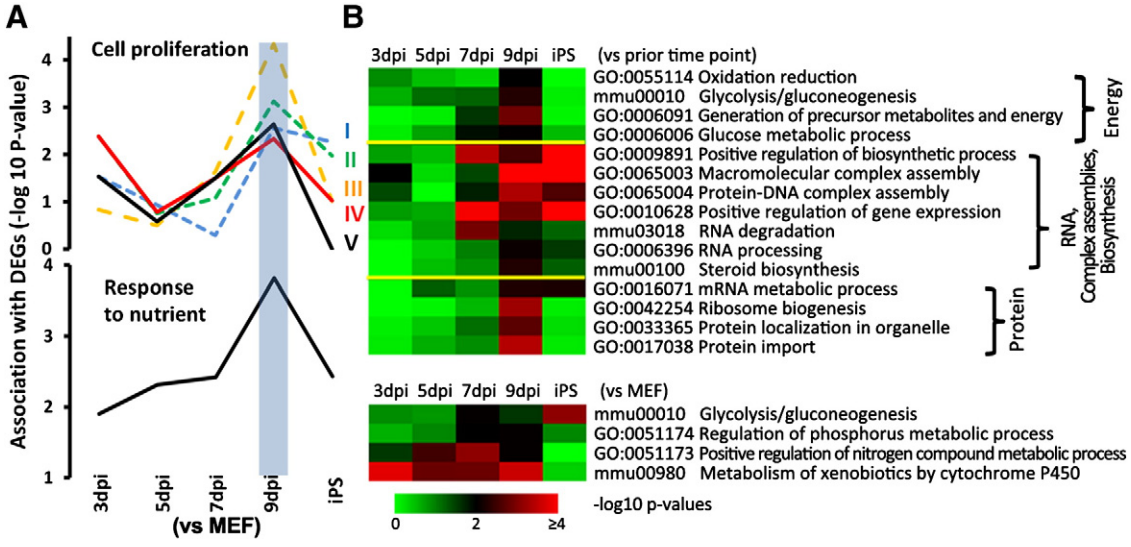

Figure 4 Regulation of ordered metabolic events. (A): Upper panel, solid line graphs depict significance of DEG regulation association with proliferation function in epithelial cell (profile IV) and mammary gland epithelial cell (profile V) from the comparisons to MEF, while three broken-lines from the comparisons to prior time-points describe similar DEG association with proliferation in general (profile III), as well as epithelial cell (profile II) and mammary gland epithelial cell proliferation (profile I); lower panel, DEG association with nutrient response functions. (B): Heat maps for the regulation of metabolism related functional gene groups during reprogramming and iPS cells.

were in line with an increase in proliferation rate during the early phase of reprogramming (Fig. 4A), a corresponding metabolic profile peaking at a late phase should exist so as to drive the biomass increase and higher energy requirements of accelerated proliferation. As expected, global metabolic activity showed such an increase peaking at 9 dpi (Fig. 4B). In further support of our view that molecular mechanisms behind accelerated cell proliferation can be deduced from regulation profiling, we found that the gene group that enables cellular response to nutrient showed significant and lasting increase in its activity (Fig. 4A) between 3 and 9 dpi (DEG association peaked at 9 dpi, $-\log$ p-values = 3.8). In providing an increase in sensitivity to nutrient and subsequent uptake so as to support rapid cell division and growth, it is an effective first indicator to subsequent metabolic reprogramming. Interestingly, we also detected significant activity of genes responding to nutrient in the fully reprogrammed iPS cells ($-\log$ p-values = 2.4) (Fig. 4A), which further attests to the differences in metabolism between pluripotent stem cells and somatic cells. Subsequent functional regulations represented a constitutive spectrum of metabolic and other associated processes. The first hint of positive nitrogen metabolism was evident at 5 dpi and by 7 dpi when glucose metabolism, phosphorus metabolism, biosynthetic and complex assembly activities were triggered. At 9 dpi, energy metabolism was highest with activated functions associated with oxidation and reduction, generation of precursor metabolites and energy, as well as glucose metabolic processes. For protein synthesis-related metabolism, we found the earliest evidence of activities at 9 dpi which included mRNA metabolism, RNA processing, ribosome biogenesis, protein transport and localization, as well as assemblies of macromolecular complexes (Fig. 4B). Although the metabolism-related genes remained significantly activated in final iPS cells after reprogramming, their activities were much lower in comparison to 9 dpi suggesting higher proliferation potential of the cells undergoing reprogramming compared to established iPS cells.

Critical role of PDGF-BB signaling during reprogramming

In order to identify key candidate factors that highly connected to DEGs, and such may influence reprogramming, we further explored DEGs obtained using a FDR threshold ≤ 0.01 (Supplementary Fig. S4) by reconstructing their temporal molecular networks using the Ingenuity Pathway Analysis (IPA) tool with missing links filled up in the process. We were particularly interested in signaling factors that function from the extracellular space which can be readily applied to cell culture system without genetic manipulation. Among several networks, we noticed that TGF-β and PDGF-BB appear commonly as central players in the networks which showed high probability scores at every time point (Fig. 5).

As the role of TGF-β has already been well known as a negative regulator in reprogramming (Ichida et al., 2009; Maherali and Hochedlinger, 2009), we investigated the effects of PDGF-BB during reprogramming. We first measured the expression levels of PDGF-A, -B and -C in CDy1^{bright} cells collected at 3, 5, 7 and 9 dpi by quantitative RT-PCR, which showed 7, 11, 58 and 67-fold increases of only PDGF-B, respectively (Fig. 6A). To figure out the role of exogenous PDGF-BB in reprogramming, we cultured OSKM-transfected Oct4-GFP MEF in a medium containing 1 ng/ml and 5 ng/ml of recombinant mouse PDGF-BB from the day after plating (3 dpi) to 24 dpi. For a strict control of the PDGF level in the medium, PDGF-free knock out serum replacement (KOSR, Life Technologies) was substituted for FBS. The number of GFP positive colonies counted at 24 dpi in 1 ng/ml PDGF and 5 ng/ml PDGF-BB treated groups was 21 ± 4 and 15 ± 3 per well whereas only 7 ± 2 colonies were observed in non-treated control wells (Fig. 6B). Because the higher PDGF-BB concentration of 5 ng/ml did not further increase the iPS cell colony numbers compared to 1 ng/ml, PDGF-BB was applied at a concentration of 1 ng/ml in the following experiments, which resulted in 3 to 6-fold increases of iPS cell generation efficiency (Figs. 6B and C). We were also able to detect significantly larger number of CDy1-positive cells in PDGF-BB treated cells starting from 7 dpi (Supplementary Fig. S5). The critical role of PDGF-BB in reprogramming was further confirmed by our finding that PDGF receptor tyrosine kinase inhibitors such as AG 17, AG 1295, AG 1296 and Imatinib mesylate (Gleevec) as well as a neutralizing antibody against PDGF-BB reduce the reprogramming efficiency (Fig. 6D). We then fractionated the PDGF-BB treatment time to determine at which time points it enhances the reprogramming efficiency. Starting from 3, 7, 11, 15 to 19 dpi, cells were treated with PDGF-BB for four consecutive days and maintained in normal culture medium until 24 dpi. The numbers of GFP positive colonies in the wells treated with PDGF-BB from 3, 7, and 11 dpi were over 2-fold higher than that of non-treated control, while the cells treated from 15 to 19 dpi generated similar numbers of colonies as the non-treated control (Fig. 6C). To assess the effect of PDGF-BB on cell proliferation rate during reprogramming we measured the size of iPS cell colonies generated in the presence and absence of PDGF-BB from 4 days before to 2 days after the expression of OCT4-GFP. The growth rates of the 2 groups of iPS cell colonies were not different (Supplementary Fig. S6). These results imply that PDGF-BB exerts its effect at early phase of reprogramming process and it is not simply due to enhanced cell proliferation.

We noted that Oct4 promoter activation, which we employed as a mean for assessing reprogramming efficiency in our study, may occur by other stimulations (Liedtke et al., 2008). To verify that the OCT4-GFP positive cell colonies grown in the medium containing PDGF-BB are iPS cells, we stained them with CDy1 and then performed immunocytochemistry with Nanog antibody. In both OCT4-GFP expressing cell colonies generated with and without PDGF-BB, Nanog staining co-localized with CDy1 as well as with GFP (Supplementary Fig. S7). Further, we randomly isolated 4 colonies and continuously passaged them for the assessment of their stemness and pluripotency. The expression of SSEA-1 was visualized by immunocytochemistry (Supplementary Fig. S8A), while the capability of differentiation into cell types of all three germ layers was demonstrated by in vivo teratoma assay (Supplementary Fig. S8B) as well as in vitro embryoid body assay (Supplementary Fig. S8C). Increased expression of endogenous OSKM factors and suppression of the exogenously introduced factors were revealed by real time RT-PCR (Supplementary Fig. S8D). We also found that the global

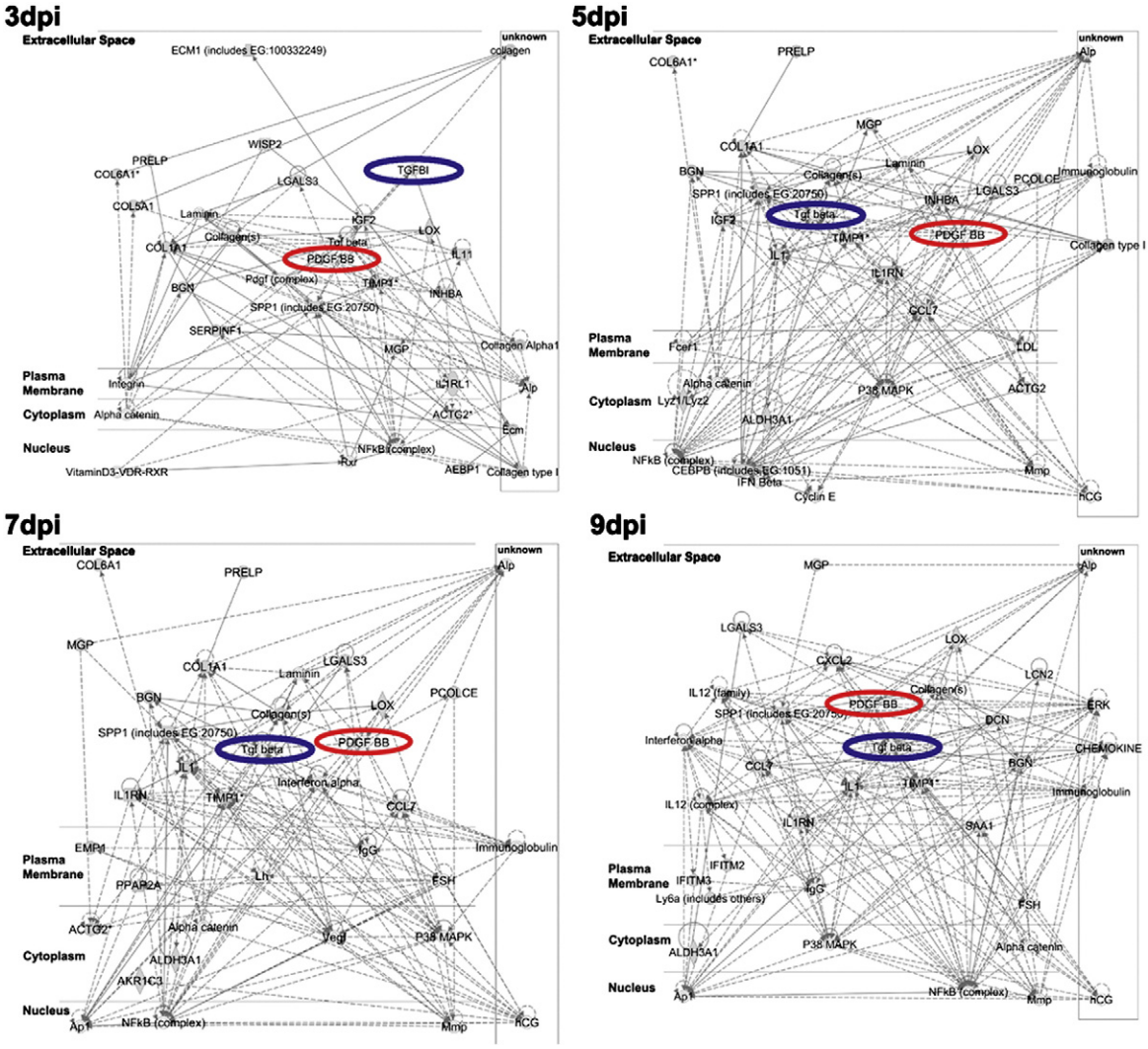

Figure 5 Network analysis with DEGs. Ingenuity Pathway Analysis networks revealed TGF-β (blue circle) and PDGF-BB (red circle) as central players that link the DEGs with a FDR threshold of 0.01.

gene expression profile of a PDGF-BB assisted iPS cell line is very similar to normal iPS and mES cell lines (Supplementary Fig. S8E and S8F).

The results of all tests demonstrated that the four cell lines are pluripotent stem cells. These results implied that the GFP expression used as a surrogate marker for reprogramming in our study is from iPS cells and the PDGF-BB treatment does not affect the normal characteristics of iPS cells.

Discussion

Through enrichment analysis as well as network analysis of DEGs, we uncovered the critical role of PDGF-BB and identified key mechanistic elements during the course of somatic cell reprogramming to iPS cells. Our analysis demonstrates how a large set of microarray data can be systematically analyzed to profile global functional regulation in a biological system. Instead of using the commonly-used fold-change, we opted to undertake global gene analysis based on corrected p-values and a corresponding FDR threshold of 0.25 in elucidating the systems biology of reprogramming. Without further gene expression validation, our threshold gives a good intuition of their global validity i.e. 75% (1−0.25), as the DEG lists are expected to have a fold-change magnitude greater than the typical gene from comparison of random profiles and a more direct translation of confidence than the common fold-change magnitude.

Determining the context-specific functions of DEGs can be challenging as individual gene analysis often results in many irrelevant possibilities of high statistical significance without further biological implication. On the other hand, the results from enrichment analysis become increasingly obvious with regard to biological significance when functionally-related groups are clustered together, or interpreted in an integrated context with other gene groups. Given that a biological function is relevant in a specific context, the sequential enrichment profile of associated gene groups can be an effective indicator of temporal regulation. This approach is well suited to the stepwise analysis of molecular and cellular events in processes such as reprogramming.

The low efficiency of somatic cell reprogramming by the expression of reprogramming factors delivered by viral vectors may be attributed to variations in transfection

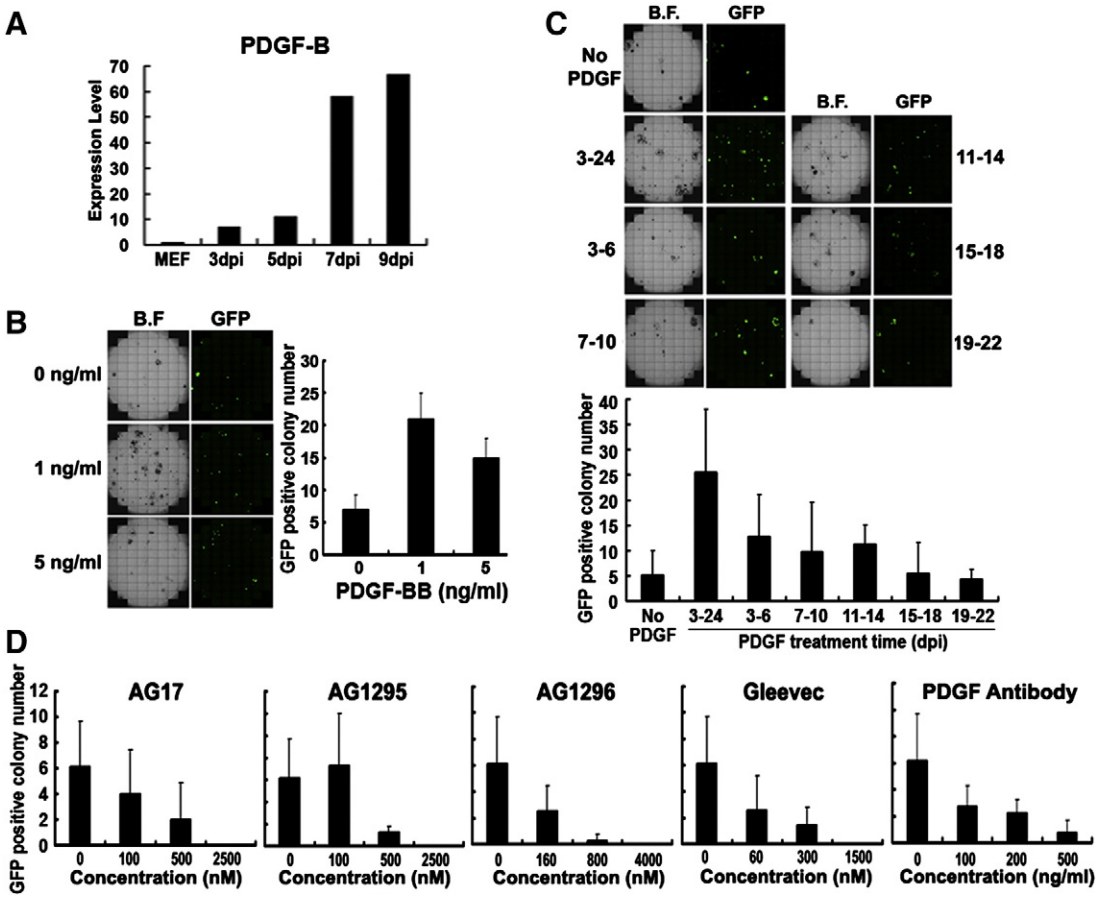

Figure 6 PDGF-BB enhances reprogramming efficiency. (A): PDGF-B gene expression levels during reprogramming measured by real time RT-PCR. (B): Microscopy images and the numbers of GFP expressing colony generated in the presence of PDGF-BB. GFP positive colonies in the wells treated with different concentrations of PDGF-BB were counted at 24 dpi. Data are presented as mean ± SD (n = 4). (C): The effect of PDGF-BB treatment at different time points of iPS cell generation. GFP positive colonies were counted at 24 dpi. Data are presented as mean ± SD (n = 4). (D): The effects of PDGFR inhibitors and PDGF antibody in reprogramming. Cells were treated from 3 dpi to 24 dpi. GFP positive colonies were counted at 24 dpi. Data are presented as mean ± SD (n = 4).

efficiency and transgene integration loci. Although the reprogramming efficiency significantly improved by drug-induced transgene expressions in genetically identical secondary MEF, it still remains as low as 4% (Wernig et al., 2008). Stochastic processes governed by factors in epigenetic regulation and cell division have been proposed to account for the different responses of each somatic cell to the reprogramming factors (Hanna et al., 2009). Despite the important role of stochasticity in reprogramming, the highly transient expression dynamics observed from our study are remarkably consistent with the robust modulation of cellular functions at critical time points. The response timings for each gene depend on its specific multi-functional roles, and the combinatorial requirements of concurrent programs. Together, genes participating in simultaneous programs may drive, coordinate, explore and respond to the reprogramming landscape, all at the same time. As such, gene expression involved can exhibit highly stochastic, complex and yet robust dynamics. As an example to illustrate the coordinated nature of reprogramming, we noted the programs regulating signaling, adhesion, cytoskeleton and extracellular matrix formation together with specific proliferation-related ones are likely to be initially activated to reset the plasticity of the transcriptome and proteome (Hansson et al., 2012), in response to OSKM activities. Subsequently, they are turned off and are distinct from the global metabolism and proliferation programs that become inbuilt later with the progression of reprogramming. The delayed proliferation programs include a rapid decline in cell size (Smith et al., 2010) and the distinct expression patterns of cell-cycle proteins (Polo et al., 2012; Ruiz et al., 2011).

PDGF has been well known to activate the PI3K/Akt pathway (Franke et al., 1995) which is involved in the stemness maintenance of both human and mouse ES cells (Armstrong et al., 2006; Pebay et al., 2005; Watanabe et al., 2006; Wong et al., 2007). Inhibition of PI3K/Akt pathway down-regulates Nanog and its target genes such as Klf4, Tbx3, and Esrrb (Storm et al., 2007, 2009) which are key factors required for self-renewal of ES cells (Ivanova et al., 2006). The addition of Tbx3 into the OSKM factors significantly improves the germ-line transmission capacity of iPS cells (Han et al., 2010) and the nuclear receptor Esrrb can substitute Klf4 in the induction of iPS cells (Feng et al., 2009a). These facts suggest that the effect of PDGF-induced PI3K/Akt signaling may be multifaceted in reprogramming. It is known that p53 suppression during reprogramming increases the reprogramming efficiency in both

human and mouse cells (Hong et al., 2009; Kawamura et al., 2009). Interestingly, we observed significant increase in Mdm2 level during reprogramming which can facilitate p53 degradation after its activation by PI3K/Akt pathway (Mayo and Donner, 2001; Ogawara et al., 2002). Hence, p53 suppression is another possible mechanism by which PDGF increases the reprogramming efficiency. As such, it is likely that signal transduction mediated by PI3K/AKT and MAPK is one fundamental mechanism involved in the enhancement of reprogramming efficiency by PDGF-BB.

Conclusions

By employing a novel method for the isolation of cells at early phases of reprogramming and taking a global perspective in interpretation of functional enrichment analysis, we uncovered a repertoire of early events during the induction of pluripotency and further identified PDGF-BB as a key player during this time. The data presented in this study will provide insight for the understanding of reprogramming mechanisms yet to be elucidated.

Acknowledgments

We thank Emmiline Ang for technical support in iPS cell generation, Tae-Hoon Chung for validating microarray data, and Bing Lim and Woon Khiong Chan for consulting on iPS cell characterization. S.-J.P., N.-Y.K., S.-W.Y. and Y.-T.C. are the inventors of the technology described in this article for which patents have been filed. This study was supported by intramural funding and a grant from Biomedical Research Council, Agency for Science, Technology and Research, Singapore (10/1/21/19/656), and a grant from the Next-Generation BioGreen 21 Program, Rural Development Administration, Republic of Korea (SSAC, No. PJ009520).

Appendix A. Supplementary data

Supplementary data to this article can be found online at http://dx.doi.org/10.1016/j.scr.2014.03.002.

References

Armstrong, L., Hughes, O., Yung, S., Hyslop, L., Stewart, R., Wappler, I., Peters, H., Walter, T., Stojkovic, P., Evans, J., et al., 2006. The role of PI3K/AKT, MAPK/ERK and NFkappabeta signalling in the maintenance of human embryonic stem cell pluripotency and viability highlighted by transcriptional profiling and functional analysis. Hum. Mol. Genet. 15, 1894–1913.

Breitling, R., Armengaud, P., Amtmann, A., Herzyk, P., 2004. Rank products: a simple, yet powerful, new method to detect differentially regulated genes in replicated microarray experiments. FEBS Lett. 573, 83–92.

Buganim, Y., Faddah, D.A., Cheng, A.W., Itskovich, E., Markoulaki, S., Ganz, K., Klemm, S.L., van Oudenaarden, A., Jaenisch, R., 2012. Single-cell expression analyses during cellular reprogramming reveal an early stochastic and a late hierarchic phase. Cell 150, 1209–1222.

Feng, B., Jiang, J., Kraus, P., Ng, J.H., Heng, J.C., Chan, Y.S., Yaw, L. P., Zhang, W., Loh, Y.H., Han, J., et al., 2009a. Reprogramming of fibroblasts into induced pluripotent stem cells with orphan nuclear receptor Esrrb. Nat. Cell Biol. 11, 197–203.

Feng, B., Ng, J.H., Heng, J.C., Ng, H.H., 2009b. Molecules that promote or enhance reprogramming of somatic cells to induced pluripotent stem cells. Cell Stem Cell 4, 301–312.

Franke, T.F., Yang, S.I., Chan, T.O., Datta, K., Kazlauskas, A., Morrison, D.K., Kaplan, D.R., Tsichlis, P.N., 1995. The protein kinase encoded by the Akt proto-oncogene is a target of the PDGF-activated phosphatidylinositol 3-kinase. Cell 81, 727–736.

Han, J., Yuan, P., Yang, H., Zhang, J., Soh, B.S., Li, P., Lim, S.L., Cao, S., Tay, J., Orlov, Y.L., et al., 2010. Tbx3 improves the germ-line competency of induced pluripotent stem cells. Nature 463, 1096–1100.

Hanna, J., Saha, K., Pando, B., van Zon, J., Lengner, C.J., Creyghton, M.P., van Oudenaarden, A., Jaenisch, R., 2009. Direct cell reprogramming is a stochastic process amenable to acceleration. Nature 462, 595–601.

Hansson, J., Rafiee, M.R., Reiland, S., Polo, J.M., Gehring, J., Okawa, S., Huber, W., Hochedlinger, K., Krijgsveld, J., 2012. Highly coordinated proteome dynamics during reprogramming of somatic cells to pluripotency. Cell Rep. 2, 1579–1592.

Hoch, R.V., Soriano, P., 2003. Roles of PDGF in animal development. Development 130, 4769–4784.

Hong, H., Takahashi, K., Ichisaka, T., Aoi, T., Kanagawa, O., Nakagawa, M., Okita, K., Yamanaka, S., 2009. Suppression of induced pluripotent stem cell generation by the p53–p21 pathway. Nature 460, 1132–1135.

Huang da, W., Sherman, B.T., Lempicki, R.A., 2009. Systematic and integrative analysis of large gene lists using DAVID bioinformatics resources. Nat. Protoc. 4, 44–57.

Ichida, J.K., Blanchard, J., Lam, K., Son, E.Y., Chung, J.E., Egli, D., Loh, K.M., Carter, A.C., Di Giorgio, F.P., Koszka, K., et al., 2009. A small-molecule inhibitor of tgf-Beta signaling replaces sox2 in reprogramming by inducing nanog. Cell Stem Cell 5, 491–503.

Im, C.N., Kang, N.Y., Ha, H.H., Bi, X., Lee, J.J., Park, S.J., Lee, S.Y., Vendrell, M., Kim, Y.K., Lee, J.S., et al., 2010. A fluorescent rosamine compound selectively stains pluripotent stem cells. Angew. Chem. Int. Ed. Engl. 49, 7497–7500.

Ivanova, N., Dobrin, R., Lu, R., Kotenko, I., Levorse, J., DeCoste, C., Schafer, X., Lun, Y., Lemischka, I.R., 2006. Dissecting self-renewal in stem cells with RNA interference. Nature 442, 533–538.

Kang, N.Y., Yun, S.W., Ha, H.H., Park, S.J., Chang, Y.T., 2011. Embryonic and induced pluripotent stem cell staining and sorting with the live-cell fluorescence imaging probe CDy1. Nat. Protoc. 6, 1044–1052.

Kawamura, T., Suzuki, J., Wang, Y.V., Menendez, S., Morera, L.B., Raya, A., Wahl, G.M., Izpisua Belmonte, J.C., 2009. Linking the p53 tumour suppressor pathway to somatic cell reprogramming. Nature 460, 1140–1144.

Laing, E., Smith, C.P., 2010. RankProdIt: a web-interactive Rank Products analysis tool. BMC Res. Notes 3, 221.

Lanner, F., Rossant, J., 2010. The role of FGF/Erk signaling in pluripotent cells. Development 137, 3351–3360.

Liedtke, S., Stephan, M., Kogler, G., 2008. Oct4 expression revisited: potential pitfalls for data misinterpretation in stem cell research. Biol. Chem. 389, 845–850.

Lin, T., Ambasudhan, R., Yuan, X., Li, W., Hilcove, S., Abujarour, R., Lin, X., Hahm, H.S., Hao, E., Hayek, A., et al., 2009. A chemical platform for improved induction of human iPSCs. Nat. Methods 6, 805–808.

Maherali, N., Hochedlinger, K., 2009. Tgfbeta signal inhibition cooperates in the induction of iPSCs and replaces Sox2 and cMyc. Curr. Biol. 19, 1718–1723.

Marion, R.M., Strati, K., Li, H., Murga, M., Blanco, R., Ortega, S., Fernandez-Capetillo, O., Serrano, M., Blasco, M.A., 2009. A p53-mediated DNA damage response limits reprogramming to ensure iPS cell genomic integrity. Nature 460, 1149–1153.

Mayo, L.D., Donner, D.B., 2001. A phosphatidylinositol 3-kinase/Akt pathway promotes translocation of Mdm2 from the cytoplasm to the nucleus. Proc. Natl. Acad. Sci. U. S. A. 98, 11598–11603.

Miki, T., Yasuda, S.Y., Kahn, M., 2011. Wnt/beta-catenin signaling in embryonic stem cell self-renewal and somatic cell reprogramming. Stem Cell Rev. 7, 836–846.

Mikkelsen, T.S., Hanna, J., Zhang, X., Ku, M., Wernig, M., Schorderet, P., Bernstein, B.E., Jaenisch, R., Lander, E.S., Meissner, A., 2008. Dissecting direct reprogramming through integrative genomic analysis. Nature 454, 49–55.

Ogawara, Y., Kishishita, S., Obata, T., Isazawa, Y., Suzuki, T., Tanaka, K., Masuyama, N., Gotoh, Y., 2002. Akt enhances Mdm2-mediated ubiquitination and degradation of p53. J. Biol. Chem. 277, 21843–21850.

Orford, K.W., Scadden, D.T., 2008. Deconstructing stem cell self-renewal: genetic insights into cell-cycle regulation. Nat. Rev. Genet. 9, 115–128.

Pebay, A., Wong, R.C., Pitson, S.M., Wolvetang, E.J., Peh, G.S., Filipczyk, A., Koh, K.L., Tellis, I., Nguyen, L.T., Pera, M.F., 2005. Essential roles of sphingosine-1-phosphate and platelet-derived growth factor in the maintenance of human embryonic stem cells. Stem Cells 23, 1541–1548.

Polo, J.M., Anderssen, E., Walsh, R.M., Schwarz, B.A., Nefzger, C. M., Lim, S.M., Borkent, M., Apostolou, E., Alaei, S., Cloutier, J., et al., 2012. A molecular roadmap of reprogramming somatic cells into iPS cells. Cell 151, 1617–1632.

Ruiz, S., Panopoulos, A.D., Herrerias, A., Bissig, K.D., Lutz, M., Berggren, W.T., Verma, I.M., Izpisua Belmonte, J.C., 2011. A high proliferation rate is required for cell reprogramming and maintenance of human embryonic stem cell identity. Curr. Biol. 21, 45–52.

Samavarchi-Tehrani, P., Golipour, A., David, L., Sung, H.K., Beyer, T. A., Datti, A., Woltjen, K., Nagy, A., Wrana, J.L., 2010. Functional genomics reveals a BMP-driven mesenchymal-to-epithelial transition in the initiation of somatic cell reprogramming. Cell Stem Cell 7, 64–77.

Silva, J., Barrandon, O., Nichols, J., Kawaguchi, J., Theunissen, T. W., Smith, A., 2008. Promotion of reprogramming to ground state pluripotency by signal inhibition. PLoS Biol. 6, e253.

Smith, Z.D., Nachman, I., Regev, A., Meissner, A., 2010. Dynamic single-cell imaging of direct reprogramming reveals an early specifying event. Nat. Biotechnol. 28, 521–526.

Storm, M.P., Bone, H.K., Beck, C.G., Bourillot, P.Y., Schreiber, V., Damiano, T., Nelson, A., Savatier, P., Welham, M.J., 2007. Regulation of Nanog expression by phosphoinositide 3-kinase-dependent signaling in murine embryonic stem cells. J. Biol. Chem. 282, 6265–6273.

Storm, M.P., Kumpfmueller, B., Thompson, B., Kolde, R., Vilo, J., Hummel, O., Schulz, H., Welham, M.J., 2009. Characterization of the phosphoinositide 3-kinase-dependent transcriptome in murine embryonic stem cells: identification of novel regulators of pluripotency. Stem Cells 27, 764–775.

Takahashi, K., Yamanaka, S., 2006. Induction of pluripotent stem cells from mouse embryonic and adult fibroblast cultures by defined factors. Cell 126, 663–676.

Utikal, J., Polo, J.M., Stadtfeld, M., Maherali, N., Kulalert, W., Walsh, R.M., Khalil, A., Rheinwald, J.G., Hochedlinger, K., 2009. Immortalization eliminates a roadblock during cellular reprogramming into iPS cells. Nature 460, 1145–1148.

Vendrell, M., Park, S.J., Chandran, Y., Lee, C.L., Ha, H.H., Kang, N. Y., Yun, S.W., Chang, Y.T., 2012. A fluorescent screening platform for the rapid evaluation of chemicals in cellular reprogramming. Stem Cell Res. 9, 185–191.

Wang, W., Yang, J., Liu, H., Lu, D., Chen, X., Zenonos, Z., Campos, L.S., Rad, R., Guo, G., Zhang, S., et al., 2011. Rapid and efficient reprogramming of somatic cells to induced pluripotent stem cells by retinoic acid receptor gamma and liver receptor homolog 1. Proc. Natl. Acad. Sci. U. S. A. 108, 18283–18288.

Watanabe, S., Umehara, H., Murayama, K., Okabe, M., Kimura, T., Nakano, T., 2006. Activation of Akt signaling is sufficient to maintain pluripotency in mouse and primate embryonic stem cells. Oncogene 25, 2697–2707.

Wernig, M., Lengner, C.J., Hanna, J., Lodato, M.A., Steine, E., Foreman, R., Staerk, J., Markoulaki, S., Jaenisch, R., 2008. A drug-inducible transgenic system for direct reprogramming of multiple somatic cell types. Nat. Biotechnol. 26, 916–924.

Wong, R.C., Tellis, I., Jamshidi, P., Pera, M., Pebay, A., 2007. Anti-apoptotic effect of sphingosine-1-phosphate and platelet-derived growth factor in human embryonic stem cells. Stem Cells Dev. 16, 989–1001.

Yoshida, Y., Takahashi, K., Okita, K., Ichisaka, T., Yamanaka, S., 2009. Hypoxia enhances the generation of induced pluripotent stem cells. Cell Stem Cell 5, 237–241.